Available online at www.sciencedirect.com
ScienceDirect
Current Opinion in Electrochemistry

Review Article

Comparative structure-potentio-spectroscopy of the *Shewanella* outer membrane multiheme cytochromes

Marcus J. Edwards, Andrew J. Gates, Julea N. Butt, David J. Richardson and Thomas A. Clarke*

Many species of bacteria can generate energy in the anoxic subsurface by directly coupling intracellular oxidative reactions to the reduction of extracellular metal oxides. Coupling these processes requires electron transfer networks that extend from the inside of the cell, across the outer membrane to the extracellular terminal electron acceptors. The best described of these networks is from *Shewanella oneidensis* MR-1, where four structures of outer membrane multiheme cytochromes (OMMCs) have been determined. These OMMCs contain 10–11 *bis*-histidine-ligated c-type hemes and are directly involved in the reduction of iron and manganese oxides at the cell surface. The heme ligands for some of these structures have been characterised using electron paramagnetic resonance (EPR), the redox properties have been mapped by protein film electrochemistry (PFE) and more recently molecular dynamic simulations have been used to obtain microscopic redox potentials for individual heme groups. This review maps these different experimental techniques onto the structures, providing insight into the intramolecular electron transfer pathways of OMMCs, revealing future directions for study.

Address
Centre for Molecular and Structural Biochemistry, School of Biological Sciences and School of Chemistry, University of East Anglia, Norwich Research Park, Norwich NR4 7TJ, United Kingdom

Corresponding author: Clarke, Thomas A. (tom.clarke@uea.ac.uk)

Current Opinion in Electrochemistry 2017, **4**:199–205

This review comes from a themed issue on **Physical & Nano-Electrochemistry**

Edited by **Feng Zhao** and **Jens Ulstrup**

For a complete overview see the Issue and the Editorial

Available online 26 August 2017

http://dx.doi.org/10.1016/j.coelec.2017.08.013

Introduction

Many bacteria can couple heterotrophic oxidation of organic matter to the reduction of terminal oxidants that substitute for molecular oxygen, a process commonly referred to as anaerobic respiration. This physiological property of bacteria is facilitated by oxidoreductase networks that oxidise quinol in the cytoplasmic membrane and relay the liberated electrons to specific terminal electron acceptor(s) [1]. The majority of *Shewanella* spp. have been shown to utilise insoluble non-diffusing terminal respiratory oxidants, namely soluble and insoluble transition metals [2,3]. Biogenic reduction of minerals is a link between carbon cycling and geochemical cycles that affect mineral formation [4,5]. Mineral reduction also affects redox processes such as methanogenesis and sulphate reduction in soil and aquatic niches [6,7], and the dissemination of many mineral-adsorbed molecules [8–11]. The final enzyme-substrate electron transfer step at the microbe–mineral interface has been shown to be dependent on the expression of multiheme cytochromes associated with the *Shewanella* outer membrane [12,13]. MtrA and MtrD are decaheme cytochromes that form putative porin-cytochrome modules (with respective β-barrels MtrB and MtrE) to relay electrons from periplasmic reductants across the outer membrane [12,14,15]. Electrons exit the porin-cytochrome complexes into outer membrane multiheme cytochromes (OMMCs) on the surface of the cell [16,17]. This review compares the spectropotentiometric and structural data available for the four major clades of OMMCs that localise to the extracellular surface of the *Shewanella* outer bacterial membrane [18–22].

Structural features of the *Shewanella* OMMC family

Shewanellacea genomes encode for multiple OMMCs with apparently similar functions. Bioinformatic analysis of *Shewanella* spp. shows that the minimal OMMCs encoded for are the decahemes MtrC and either OmcA or UndA [23]. MtrC has been extensively characterised for its affinity to the MtrAB complex and its canonical role as a mineral reductase [15,16]. MtrF has been identified as a component of the paralogous MtrDEF heterotrimer, which is up-regulated in aerobic *S. oneidensis* MR-1 biofilms [24]. A lipid anchor maintains OmcA's outer membrane localisation, and its mineral reduction activity is dependent on its association to MtrCAB [13,25,26]. A comprehensive gene knock-out study determined that the presence of either *mtrC* or *omcA* in the *S. oneidensis* genome maintained significant wild-type iron oxide reduction [13]. Known mineral-reducing *Shewanella* species that do not have *omcA* in their genomes encode for UndA, an undecaheme cytochrome indicated to have an analogous

Figure 1

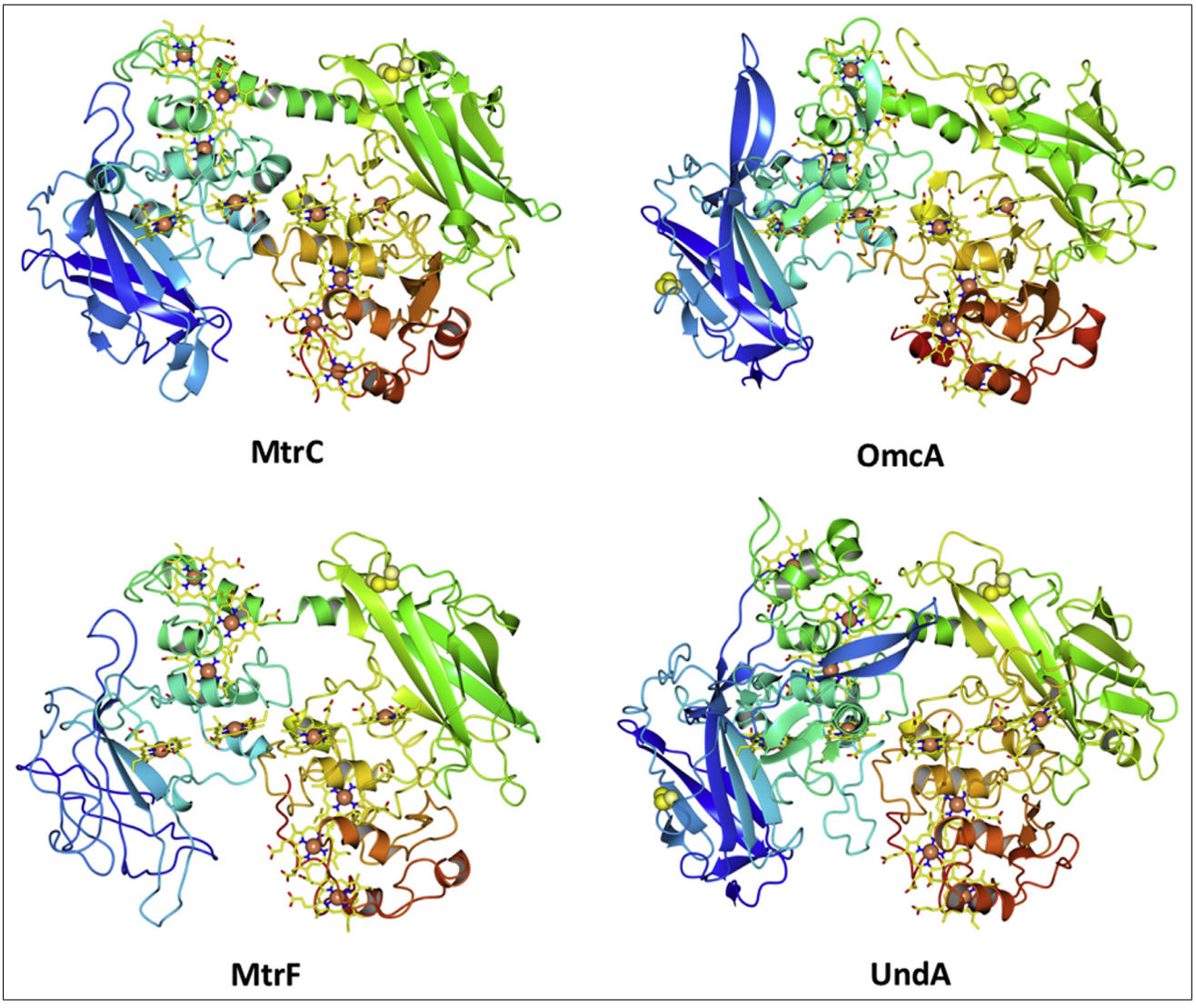

Crystal structures of MtrC [30], MtrF [27], OmcA [28] of *Shewanella oneidensis* MR-1 and UndA [29] of *Shewanella* sp. Strain HRCR-6. Polypeptide chains are shown in cartoon representation and coloured from blue (N-terminus) to red (C-terminus). Hemes are shown in stick representation with the iron atoms shown as orange spheres.

role to OmcA because it is capable of complementing ferrihydrite reduction in *mtrC*$^{-}$*omcA*$^{-}$ *S. oneidensis* MR-1 [22].

The molecular structures of representatives of each of the four OMMC clades in *Shewanella* have been determined: the decaheme MtrF, OmcA and MtrC of *S. oneidensis* and the undecaheme UndA of *S.* HRCR-6 (Figure 1) [27–30••]. All structures are formed of four domains, two multiheme domains that are flanked by two β-barrels with β-strands arranged in Greek key motifs. MtrF, OmcA and MtrC contain a conserved decaheme 'staggered cross' cofactor arrangement, with UndA containing an 11th heme that is inserted between hemes 6 and hemes 7 in the amino acid sequence. The staggered cross heme arrangement means there are four potential sites for electrons to enter and exit the structure, with two opposing ends of the cross pointing into the β-barrels and two exposed at the edges of the multiheme domains. The structures also reveal a conserved $CX_{8-15}C$ disulphide within the β-barrel of domain III. A second $CX_{2-3}C$ disulphide is in UndA, OmcA and a subpopulation of MtrC located within the N-terminal β-barrel domain I; this CX_3C motif is present in the amino acid sequence of MtrF but the putative disulphide bond was not resolved due to poor electron density in that domain. There is appreciable structural conservation of OMMC domains, as well as significant maintenance of heme positioning, despite less than 25%

sequence homology between the least divergent clade members [28,30].

The comparative spectropotentiometric properties of the OMMCs

The internal molecular landscape of the OMMCs is likely to lead to distinct energy landscapes and subsequently different redox properties of the proteins. Protein film electrochemistry (PFE) provides high-resolution potentiometric data of electrode-adsorbed protein [31]. The OMMCs are lipoproteins and it could be argued that protein in solution mimics their molecular environment best, although it is equally noted that molecular crowding at a densely packed membrane surface with an insoluble substrate may be better reproduced by adsorbing a protein to an electrode [32]. As such, the advantage of high-resolution data comes at the expense of a possibility that some proteins may have different potentiometric properties in solution than when surface adsorbed. The PFE of the four OMMCs provides very accurate, high-resolution characterisation of the cytochromes' oxidation state that highlights their different redox potential behaviour (Figure 2) [27,33,34]. For each cytochrome a representative reducing and oxidising scan is plotted, where the respective negative and positive Faradaic responses correspond to the protein performing electron transfer to (positive response) and from (negative response) the working electrode during cyclic voltammetry (CV). Each OMMC voltammogram was successfully confirmed to have peaks that remained unchanged during rapid electrode rotation and a change of buffer, confirming adsorbed species were producing the voltammetric responses observed. The redox potentials of the OMMC are broadly similar, although MtrC contains a population of hemes that are at a higher potential than the other OMMC and lacks the lower potential hemes present for the other OMMC. The hemes of MtrF cover a broad range of potentials, and includes a small population of hemes that correlate to approximately ≥ -250 mV vs standard hydrogen electrode. Previously, the potential window of MtrC was shown to be higher than OmcA, with apparent midpoint potentials and window of -138 ± 275 mV for MtrC and -175 ± 300 mV for OmcA reported at pH 6 at 4 °C on graphite electrodes [35]. Despite the differences in potential, the overlapping potential windows of MtrC and OmcA indicate that reversible electron exchange between the two OMMC, in particular MtrC and OmcA, is possible.

EPR-monitored potentiometric titres provide information on specific heme populations, based on the spectroscopic resolution of heme populations that can be correlated to their respective OMMC crystal structure. Low spin, ferric heme has one unpaired 3*d* valence electron; whereas ferrous heme has zero unpaired valence electrons. Thus, EPR potentiometric titrations can monitor the redox transformations of the OMMC *c*-type hemes from their resonating, oxidised $S = \frac{1}{2}$ state to their EPR-silent reduced $S = 0$ state. To date, MtrC, MtrF and OmcA potentiometric data have been published [27,33]. The oxidised EPR spectra of MtrF and MtrC are characteristic of low spin ($S = ½$) ferric heme populations grouped into two clusters, denoted LS (i.e., low spin) or LGM (i.e., large g_{max}) (Figure 3). Near-perpendicular *bis*-histidine ligand heme rings result in increased rhombicity of LGM signals which thus appear on the low field side of the LS signals at $g_1 \approx 3.7 - 3.1$ [36]. The LS signals are rhombic signals (i.e., $3.1 > g_1 > 2.5$) characteristic of low spin fer-

Figure 2

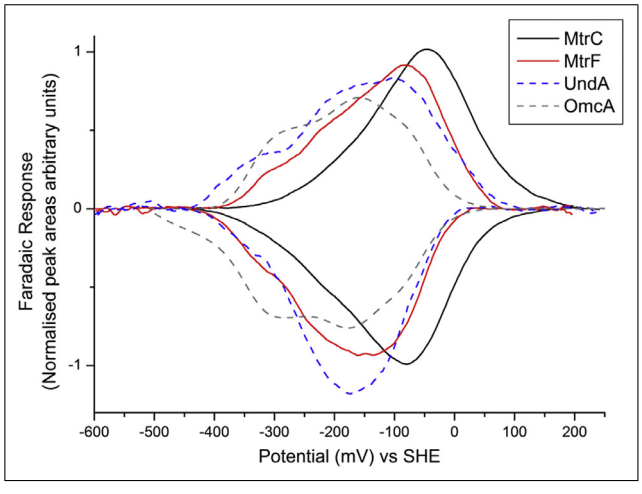

Protein film electrochemistry of extracellular cytochromes. Cyclic voltammetry of MtrC (black line), pH 7.6 [15], MtrF (red line), pH 7.0 [27], OmcA (grey dash), pH 7.4 [34] and UndA (blue dash), pH 7, measured at 30 mV/s in 25 mM HEPES, 100 mM NaCl.

Figure 3

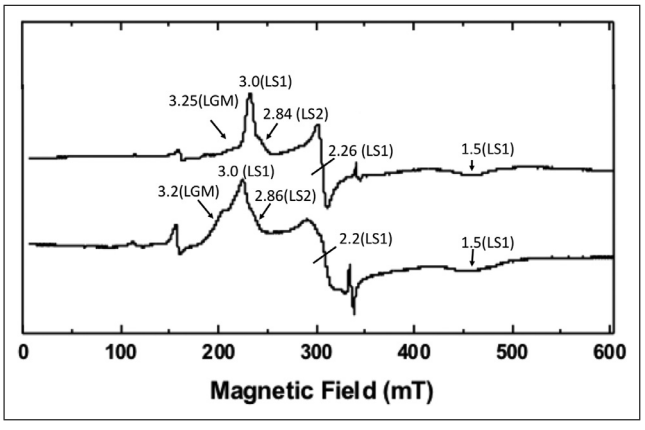

Continuous wave EPR spectra of 140 μM MtrC (upper) and 95 μM MtrF (lower) in 50 mM HEPES, 100 mM NaCl, 0.5% CHAPS [27,33]. EPR recorded using a Bruker ER100 EPR spectrometer at 10 K using 9.68 GHz frequency, 10-G modulation amplitude and 2 mW power. Low spin (LS1 and LS2) and large g_{max} (LGM) signals are indicated in parentheses next to their corresponding *g*-values.

Figure 4

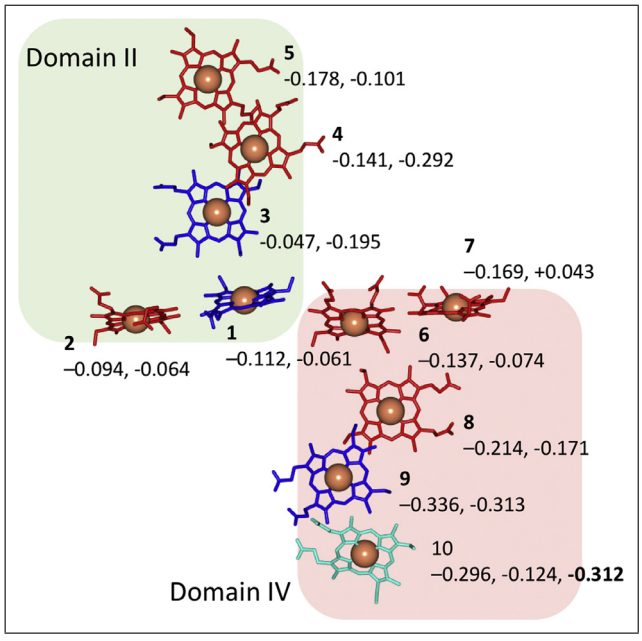

The structural arrangement of MtrF hemes. Hemes of domain II and IV are shown within blue and red boxes, respectively. Hemes with near-perpendicular *bis*-histidine ligation that would give LGM EPR signals ($\varphi_{bH} \geq 45°$) are shown in blue. Near-parallel *bis*-histidine ligated that would give LS1 EPR signals ($\varphi_{bH} \leq 45°$) are shown in red. Heme 10, that is likely to give an imidazolate histidine based on the crystal structure and generate an LS2 EPR signal, is shown in cyan. Each heme has assigned microscopic redox potentials that correspond to single-electron reduction of a fully oxidised MtrF. Microscopic redox potentials are from Wanatabe *et al.* (left [38]) and Breuer *et al.* (right [39]). The macroscopic heme potential determined for heme 10 is shown in bold [27]. Heme potentials values shown in volts.

ric hemes with decreased rhombicity, such as near-parallel *bis*-imidazole rings (i.e., $g_1 \approx 3.0 - 2.9$). The EPR spectrum of OmcA contained a signal attributed to a population of high spin heme in addition to both LS and LGM signals [37]. However, the crystal structure of OmcA revealed that all 10 heme groups were low spin, suggesting that the observed high spin signal could be due to a small population of high spin hemes within the sample, possibly originating from denatured protein.

It is possible to tentatively assign resonance signals to specific structural heme populations in the oxidised OMMCs in conjunction with the *bis*-histidine ring dihedral angle (φ_{bH}) data available from the published crystal structures (Figure 4). The published EPR spectrum of MtrC contains three resonance populations, including LGM ($g_1 \approx 3.2$), and two low spin: LS1 ($g_1 \approx 3.0$) and LS2 ($g_1 \approx 2.86$) (Figure 3). Spin quantitation was not reported in this study, and so resonance populations cannot be attributed to structural hemes although the propionate group of heme 6 may deprotonate its own distal His^{500} ligand, producing the low potential LS2 signal. LS1 appears to be the dominant resonance population by g_1 peak height. However, the double integral of the LGM signal, that has a comparable g_1 peak height to the LS1 signal and must have a larger magnetic field coverage, is directly proportional to spin concentration and may be larger in MtrC. This would reflect the distribution of φ_{bH} amongst MtrC's hemes: excluding the putative LS2 heme 6, there are four LGM candidate hemes and six LS1 candidates.

Spin quantitation of the EPR spectrum of oxidised MtrF reported 7.86 spins per protein split into three different resonance signals. The quantitation of less than 10 spins per oxidised MtrF was attributed to possible dipolar resonance coupling between hemes [27]. The predominantly low φ_{bH} of MtrF's hemes is reflected in the EPR spectrum, which accounts for five to six LS1 hemes of the six crystallographically observed (i.e., hemes 2, 4, 5, 6, 7 and 8; $g_{1,2,3} = 3.0$, 2.26, and 1.5) (Figure 3). Two of the three near-perpendicular *bis*-histidine-ligated hemes (i.e., hemes 1, 3, 9; $g_{1,2,3} = 3.25$, 2.02, and 1.15) are accounted for in spin quantitation of MtrF's LGM resonance signal. The histidinate-ligated heme 10 is attributed to producing LS2 resonance ($g_{1,2,3} = 2.84$, 2.31, and 1.63). The LS1 heme population of near-parallel hemes titrate over a broad potential window, 0 to −250 mV vs S.H.E., and the g_1 peak height dominated the oxidised EPR spectrum, further supporting the origin of the signal from multiple hemes. The broad $g_1 = 3.26$ LGM signal is produced by near-perpendicular *bis*-histidine ligand pairs (hemes 1, 3, or 9) although signal quantitation only accounts for two of these LGM hemes titrating between −100 and −260 mV. The LS2 signal (i.e., $g_1 = 2.84$) originating from ferric heme with an imidazolate ligand amounts to a single heme (i.e., heme 10), the only signal remaining at −260 mV. As such heme 10 is putatively the lowest potential heme of MtrF. This correlates well with the PFV, which also identified a low potential heme at −250 mV.

Large-scale molecular dynamic simulations have attempted to resolve the electron transport network through the ten hemes of the MtrF molecular structure. Microscopic redox potentials for the single-electron reduction of each individual heme, with the other nine hemes in the oxidised states (i.e., oxidised MtrF) have been reported by two groups [38,39] (Figure 4). Breuer *et al.* [39] suggested that the potentials of the heme pairs across the two pentaheme domains were similar, allowing for bidirectional electron transfer pathways across MtrF. Watanabe *et al.* [38] alternatively proposed that the heme potentials in domain IV were lower than in domain II, suggesting a downhill electron transfer path from domain IV to domain II. Both studies identified the heme potentials in hemes 2 and 7 as being suitable for electron transfer to flavin groups and suggested heme 9 as being the lowest potential heme group, as opposed to heme 10 that was inferred from the crystal structure. This may be due to

the challenges of accurately modelling a low-resolution MtrF structure, and it will be interesting to compare similar studies on the high-resolution MtrC structure in the future.

The interaction of flavins and OMMCs

S. oneidensis secretes both riboflavin and flavin mononucleotide (FMN) and these secreted flavins have a substantial impact on the ability of *S. oneidensis* to reduce Fe(III) oxides [40]. One hypothesis is that both riboflavin and FMN function as soluble redox mediators that facilitate electron exchange between *S. oneidensis* and solid metal oxides [41]. This is supported by studies that identified a *bfe* gene in *S. oneidensis* that was essential both for secretion of flavin into the extracellular medium and the ability of *S. oneidensis* to reduce Fe(III) oxides [42•]. As both *bfe* and *mtr* are important for extracellular electron transfer it is likely that flavins must interact with either directly or indirectly with extracellular OMMC on the cell surface. Dissociation constants of 29 μM and 255 μM between oxidised FMN and oxidised MtrC or OmcA, respectively, have been measured [43]. Given that the *S. oneidensis* extracellular FMN concentration does not exceed 1 μM during growth, these dissociation constants suggest a transient interaction between FMN and the OMMC. However, electrochemical and voltammetric studies on *S. oneidensis* biofilms generated on the surface of electrodes indicated that under anaerobic conditions MtrC associated with FMN to produce a semi-reduced flavin at the biofilm–flavin interface, suggesting the formation of a MtrC-FMN complex [44,45•]. These different results could be harmonised if the interaction between MtrC and FMN was different under aerobic and anaerobic respiratory conditions. Accordingly, a reversible transition of MtrC between cytochrome and flavocytochrome states that is controlled by the redox state of a conserved disulphide has been reported [30]. *S. oneidensis* strains that are unable to form the disulphide were severely compromised in their ability to grow aerobically, but not anaerobically, suggesting that the MtrC-FMN flavocytochrome may reduce oxygen and produce reactive oxygen species, so its formation must be closely regulated during life at oxic–anoxic interfaces. This indicates that the flavin must bind within the proximity of conserved disulphide and close enough to one or more heme groups to support electron transfer at catalytic rate. For OmcA mutation of the distal axial ligand of heme 7 in OmcA has been shown to lower the affinity of OmcA for FMN, indicating a similar interaction [46]. Different groups have utilised molecular dynamic simulations to identify riboflavin and FMN binding sites on OMMC [43,47•,48•]. Most recently two sites capable of binding riboflavin FMN binding sites were identified on OmcA close to hemes 5 and 7, while up to four possible binding sites were identified on MtrC close to hemes 1, 4, 7 and 9 [49••]. The experimental data support the binding of two flavin molecules to OmcA, and only one to MtrC, so it is still unclear which of these MD simulations best supports the experimental data.

Conclusion

The four X-ray crystal structures of representative members of each of the four clades of OMMC published over the last 6 years have provided a molecular foundation for many research groups to study the electrochemical properties of these proteins, both experimentally and through theoretical models. Much remains to be understood though, notably the precise nature of flavin binding to the OMMCs and the structures of the complexes with which the OMMCs interact in order to receive electrons from inside the cell at the cell surface. Functional MtrCAB complexes that catalyses trans-outer membrane electron transfer in proteoliposomes have given some insight into this process, but further progress on a molecular understanding that might underpin further electrochemical insights will benefit from a high-resolution structure of the complex.

Acknowledgement

This research was supported by the Biotechnology and Biological Sciences Research Council (BB/K009885/1, BB/L023733/1, BB/H07288/1).

References and recommended reading

Papers of particular interest, published within the period of review, have been highlighted as:

- •Paper of special interest
- ••Paper of outstanding interest.

1. Richardson DJ: **Bacterial respiration: a flexible process for a changing environment**. *Microbiology-Sgm* 2000, **146**:551–571.
2. Nealson KH, Myers CR: **Microbial reduction of manganese and iron—new approaches to carbon cycling**. *Appl Environ Microbiol* 1992, **58**:439–443.
3. Myers CR, Nealson KH: **Bacterial manganese reduction and growth with manganese oxide as the sole electron-acceptor**. *Science* 1988, **240**:1319–1321.
4. Fredrickson JK, Zachara JM, Kennedy DW, Liu CX, Duff MC, Hunter DB, Dohnalkova A: **Influence of Mn oxides on the reduction of uranium(VI) by the metal-reducing bacterium *Shewanella putrefaciens***. *Geochim Cosmochim Acta* 2002, **66**:3247–3262.
5. Kukkadapu RK, Zachara JM, Fredrickson JK, Kennedy DW: **Biotransformation of two-line silica-ferrihydrite by a dissimilatory Fe(III)-reducing bacterium: formation of carbonate green rust in the presence of phosphate**. *Geochim Cosmochim Acta* 2004, **68**:2799–2814.
6. Ponnamperuma FN, Brady NC: **The chemistry of submerged soils**, Volume 24. In *Advances in Agronomy*: Academic Press; 1972:29–96.
7. Presley BJ, Nissenba A, Kaplan IR, Kolodny Y: **Early diagenesis in a reducing fjord, Saanich inlet, British Columbia 0.2. Trace element distribution in interstitial water and sediment**. *Geochim Cosmochim Acta* 1972, **36**:1073.
8. Mortimer CH: **The exchange of dissolved substances between mud and water in lakes**. *J Ecol* 1941, **29**:280–329.
9. Nealson KH, Belz A, McKee B: **Breathing metals as a way of life: geobiology in action**. *Antonie Van Leeuwenhoek Int J Gen Mol Microbiol* 2002, **81**:215–222.

10. Reyes C, Murphy JN, Saltikov CW: **Mutational and gene expression analysis of mtrDEF, omcA and mtrCAB during arsenate and iron reduction in *Shewanella* sp. ANA-3**. *Environ Microbiol* 2010, **12**:1878–1888.

11. White GF, Edwards MJ, Gomez-Perez L, Richardson DJ, Butt JN, Clarke TA: **Mechanisms of bacterial extracellular electron exchange**. *Adv Microb Physiol* 2016, **68**:87–138.

12. Coursolle D, Baron DB, Bond DR, Gralnick JA: **The Mtr respiratory pathway is essential for reducing flavins and electrodes in *Shewanella oneidensis***. *J Bacteriol* 2010, **192**:467–474.

13. Coursolle D, Gralnick JA: **Modularity of the Mtr respiratory pathway of *Shewanella oneidensis* strain MR-1**. *Mol Microbiol* 2010, **77**:995–1008.

14. Dohnalkova AC, Marshall MJ, Arey BW, Williams KH, Buck EC, Fredrickson JK: **Imaging hydrated microbial extracellular polymers: comparative analysis by electron microscopy**. *Appl Environ Microbiol* 2011, **77**:1254–1262.

15. Hartshorne RS, Reardon CL, Ross D, Nuester J, Clarke TA, Gates AJ, Mills PC, Fredrickson JK, Zachara JM, Shi L, et al.: **Characterization of an electron conduit between bacteria and the extracellular environment**. *Proc Natl Acad Sci USA* 2009, **106**:22169–22174.

16. Reardon CL, Dohnalkova AC, Nachimuthu P, Kennedy DW, Saffarini DA, Arey BW, Shi L, Wang Z, Moore D, McLean JS, et al.: **Role of outer-membrane cytochromes MtrC and OmcA in the biomineralization of ferrihydrite by *Shewanella oneidensis* MR-1**. *Geobiology* 2010, **8**:56–68.

17. White GF, Shi Z, Shi L, Wang ZM, Dohnalkova AC, Marshall MJ, Fredrickson JK, Zachara JM, Butt JN, Richardson DJ, et al.: **Rapid electron exchange between surface-exposed bacterial cytochromes and Fe(III) minerals**. *Proc Natl Acad Sci USA* 2013, **110**:6346–6351.

18. Myers CR, Myers JM: **Cell surface exposure of the outer membrane cytochromes of *Shewanella oneidensis* MR-1**. *Lett Appl Microbiol* 2003, **37**:254–258.

19. Myers CR, Myers JM: **Location of cytochromes to the outer-membrane of anaerobically grown *Shewanella putrefaciens* MR-1**. *J Bacteriol* 1992, **174**:3429–3438.

20. Shi L, Deng S, Marshall MJ, Wang ZM, Kennedy DW, Dohnalkova AC, Mottaz HM, Hill EA, Gorby YA, Beliaev AS, et al.: **Direct involvement of type II secretion system in extracellular translocation of *Shewanella oneidensis* outer membrane cytochromes MtrC and OmcA**. *J Bacteriol* 2008, **190**:5512–5516.

21. Donald JW, Hicks MG, Richardson DJ, Palmer T: **The c-type cytochrome OmcA localizes to the outer membrane upon heterologous expression in *Escherichia coli***. *J Bacteriol* 2008, **190**:5127–5131.

22. Shi L, Belchik SM, Wang Z, Kennedy DW, Dohnalkova AC, Marshall MJ, Zachara JM, Fredrickson JK: **Identification and characterization of UndA(HRCR-6), an outer membrane endecaheme c-type cytochrome of *Shewanella* sp. strain HRCR-6**. *Appl Environ Microbiol* 2011, **77**:5521–5523.

23. Fredrickson JK, Romine MF, Beliaev AS, Auchtung JM, Driscoll ME, Gardner TS, Nealson KH, Osterman AL, Pinchuk G, Reed JL, et al.: **Towards environmental systems biology of *Shewanella***. *Nat Rev Microbiol* 2008, **6**:592–603.

24. McLean JS, Pinchuk GE, Geydebrekht OV, Bilskis CL, Zakrajsek BA, Hill EA, Saffarini DA, Romine MF, Gorby YA, Fredrickson JK, et al.: **Oxygen-dependent autoaggregation in *Shewanella oneidensis* MR-1**. *Environ Microbiol* 2008, **10**:1861–1876.

25. Zhang H, Tang X, Munske GR, Zakharova N, Yang L, Zheng C, Wolff MA, Tolic N, Anderson GA, Shi L, et al.: **In vivo identification of the outer membrane protein omcA-mtrC interaction network in *Shewanella oneidensis* MR-1 cells using novel hydrophobic chemical cross-linkers**. *J Proteome Res* 2008, **7**:1712–1720.

26. Ross DE, Ruebush SS, Brantley SL, Hartshorne RS, Clarke TA, Richardson DJ, Tien M: **Characterization of protein–protein interactions involved in iron reduction by *Shewanella oneidensis* MR-1**. *Appl Environ Microbiol* 2007, **73**:5797–5808.

27. Clarke TA, Edwards MJ, Gates AJ, Hall A, White GF, Bradley J, Reardon CL, Shi L, Beliaev AS, Marshall MJ, et al.: **Structure of a bacterial cell surface decaheme electron conduit**. *Proc Natl Acad Sci USA* 2011, **108**:9384–9389.

28. Edwards MJ, Baiden NA, Johs A, Tomanicek SJ, Liang L, Shi L, Fredrickson JK, Zachara JM, Gates AJ, Butt JN, et al.: **The X-ray crystal structure of *Shewanella oneidensis* OmcA reveals new insight at the microbe–mineral interface**. *FEBS Lett* 2014, **588**:1886–1890.

29. Edwards MJ, Hall A, Shi L, Fredrickson JK, Zachara JM, Butt JN, Richardson DJ, Clarke TA: **The crystal structure of the extracellular 11-heme cytochrome UndA reveals a conserved 10-heme motif and defined binding site for soluble iron chelates**. *Structure* 2012, **20**:1275–1284.

30. •• Edwards MJ, White GF, Norman M, Tome-Fernandez A, Ainsworth E, Shi L, Fredrickson JK, Zachara JM, Butt JN, Richardson DJ, et al.: **Redox linked flavin sites in extracellular decaheme proteins involved in microbe–mineral electron transfer**. *Sci Rep*, vol 5 2015. Article number 11677.

This paper describes the crystal structure of MtrC and also identifies conditions for tight flavin binding.

31. Leger C, Bertrand P: **Direct electrochemistry of redox enzymes as a tool for mechanistic studies**. *Chem Rev* 2008, **108**:2379–2438.

32. Edited by Butt J: **Voltammetry of adsorbed proteins**: *Encyclopedia of Applied Electrochemistry*. Edited by Kreysa G, Ota K-i, Savinell RF. New York: Springer; 2014:2103–2109.

33. Hartshorne RS, Jepson BN, Clarke TA, Field SJ, Fredrickson J, Zachara J, Shi L, Butt JN, Richardson DJ: **Characterization of *Shewanella oneidensis* MtrC: a cell-surface decaheme cytochrome involved in respiratory electron transport to extracellular electron acceptors**. *J Biol Inorg Chem* 2007, **12**:1083–1094.

34. Hwang ET, Orchard KL, Hojo D, Beton J, Lockwood CW, Adschiri T, Butt JN, Reisner E, Jeuken LJC: **Exploring step-by-step assembly of nanoparticle: cytochrome biohybrid photoanodes**. *ChemElectroChem* 2017, **4**:1–11.

35. Firer-Sherwood M, Pulcu GS, Elliott SJ: **Electrochemical interrogations of the Mtr cytochromes from *Shewanella*: opening a potential window**. *J Biol Inorg Chem* 2008, **13**:849–854.

36. Walker FA, Huynh BH, Scheidt WR, Osvath SR: **Models of the cytochromes *b*. Effect of axial ligand plane orientation on the EPR and Mössbauer-spectra of low-spin ferrihemes**. *J Am Chem Soc* 1986, **108**:5288–5297.

37. Bodemer GJ, Antholine WA, Basova LV, Saffarini D, Pacheco AA: **The effect of detergents and lipids on the properties of the outer-membrane protein OmcA from *Shewanella oneidensis***. *J Biol Inorg Chem* 2010, **15**:749–758.

38. Watanabe HC, Yamashita Y, Ishikita H: **Electron transfer pathways in a multiheme cytochrome MtrF**. *Proc Natl Acad Sci USA* 2017, **114**:2916–2921.

39. Breuer M, Zarzycki P, Blumberger J, Rosso KM: **Thermodynamics of electron flow in the bacterial deca-heme cytochrome MtrF**. *J Am Chem Soc* 2012, **134**:9868–9871.

40. Marsili E, Baron DB, Shikhare ID, Coursolle D, Gralnick JA, Bond DR: ***Shewanella* secretes flavins that mediate extracellular electron transfer**. *Proc Natl Acad Sci USA* 2008, **105**:3968–3973.

41. Brutinel ED, Gralnick JA: **Shuttling happens: soluble flavin mediators of extracellular electron transfer in *Shewanella***. *Appl Microbiol Biotechnol* 2012, **93**:41–48.

42. • Kotloski NJ, Gralnick JA: **Flavin electron shuttles dominate extracellular electron transfer by *Shewanella oneidensis***. *MBio* 2013, **4**:e00553-12.

This paper shows explicitly that flavin secretion plays an important role in *S. oneidensis* reduction of minerals and electrodes.

43. Paquete CM, Fonseca BM, Cruz DR, Pereira TM, Pacheco I, Soares CM, Louro RO: **Exploring the molecular mechanisms of electron shuttling across the microbe/metal space**. *Front Microbiol* 2014, **5**:318.

44. Okamoto A, Hashimoto K, Nealson KH, Nakamura R: **Rate enhancement of bacterial extracellular electron transport involves bound flavin semiquinones**. *Proc Natl Acad Sci USA* 2013, **110**:7856–7861.

45. • Okamoto A, Kalathil S, Deng X, Hashimoto K, Nakamura R, Nealson KH: **Cell-secreted flavins bound to membrane cytochromes dictate electron transfer reactions to surfaces with diverse charge and pH**. *Sci Rep* 2014, **4**:5628.
This paper was the first to indicate the *in vivo* presence of reactive flavin-cytochrome complexes on the surface of *S. oneidensis*.

46. Neto SE, de Melo-Diogo D, Correia IJ, Paquete CM, Louro RO: Characterization of OmcA mutants from *Shewanella oneidensis* MR-1 to investigate the molecular mechanisms underpinning electron transfer across the microbe–electrode interface. *Fuel Cells*: in press, http://dx.doi.org/10.1002/fuce.201700023.

47. • Breuer M, Rosso KM, Blumberger J: **Flavin binding to the deca-heme cytochrome MtrC: insights from computational molecular simulation**. *Biophys J* 2015, **109**:2614–2624.
This paper suggests likely models of flavin docking onto the surface of MtrC.

48. • Hong G, Pachter R: **Bound flavin-cytochrome model of extracellular electron transfer in *Shewanella oneidensis*: analysis by free energy molecular dynamics simulations**. *J Phys Chem B* 2016, **120**:5617–5624.
This simulation paper looks at the theoretical changes in heme iron potential within MtrC.

49. •• Babanova S, Matanovic I, Cornejo J, Bretschger O, Nealson K, Atanassov P: **Outer membrane cytochromes/flavin interactions in *Shewanella* spp.—a molecular perspective**. *Biointerphases*, vol 12 2017 021004.
This recent molecular dynamics simulation looks at possible binding sites for flavin on the surfaces of the *S. oneidensis* OMMC.